Evolutionary Optimization Algorithms in Designing a UPFC Based POD Controller

Anwar Haider
University of Bahrain
Department of Mechanical Engineering
University of Bahrain - Isa Town
Bahrain
aakabhar@uob.edu.bh

Ali Al-Mawsawi
University of Bahrain
Department of Electrical and Electronics Engineering
University of Bahrain - Isa Town
Bahrain
aalmossawi@uob.edu.bh

Ahmed Al-Qallaf
University of Bahrain
Department of Electrical and Electronics Engineering
University of Bahrain - Isa Town
Bahrain
saa-1985@hotmail.com

Abstract: This paper investigates the design of a unified power flow controller (UPFC) based power oscillations damping (POD) controller using evolutionary optimization algorithms (EA). It introduces two optimization algorithms: biogeography based optimization (BBO) and particle swarm optimization (PSO), that are used to design the POD controllers. The optimal set of parameters for the controllers are found using two different objective functions, eigenvalue based objective function and time based objective function, over a wide range of system operating points in order to obtain a robust controller. The obtained controllers are then verified and tested over four different loading conditions of the system with different system parameter uncertainties introduced in each case.

Key–Words: Power system oscillations, unified power flow controller, biogeography based optimization, particle swarm optimization, evolutionary optimization algorithms, FACTS

1 Introduction

Due to the continuous urban and industrial developments in many parts in the world in the recent years, the demands on power have increased dramatically. This led to tremendous increase in size and complexity of interconnection of power systems and networks to meet this surging demand of power.

The interconnection of remote power networks usually introduce low frequency oscillations in the range of 0.1~3.0 Hz[1]. The oscillatory modes in these systems results in degradation of the overall performance of the systems, which necessitates introduction of damping factor to avoid their excessive growth which could eventually lead to loss of synchronism [1, 2].

The Limitations of the transmission systems are handled and improved through the use of FACTS devises. These devices are utilized usually to solve problems associated with steady state phase of power network response, through controlling the transmission system parameter to force it operate in the vicinity of its thermal limits. Comparing to power system stabilizers (PSS) which can cause significant variations in voltage profile and hence may result in leading power factor under severe disturbances [3]. FACTS controllers exhibit superior performance in the transient characteristic of power systems. So, FACTS controllers in known to provide better solution in damping power system oscillation over PSS.

Wang in [4], introduced a unified model for FACTS devices that can be incorporated in Philips-Heffron model for power system oscillation studies. The study has investigated the capabilities of Static Var Compensator (SVC), Controllable Series Compensator (CSC), and Phase Shifters (PS) to damp power system oscillations in an SMIB system.In [3], a coordinated control of PSS and SVC was introduced. Several references in literatures have investigated the capability of the Thyristor Controlled Series Capacitor (TCSC) to damp the power system oscillations through different approaches, have been the focus of investigation of several literatures and publications.

STATCOM capability to damp power system oscillations was superior to that of SVC [5]. Singular value decomposition (SVD) approach in investigate the controllability of poorly damped electromechanical modes via STATCOM input channels was introduced and presented in [6].

Being the most versatile FACTS controller, the UPFC had become an interesting field of research for damping power system oscillations. In [7], a UPFC based stabilizer was developed to mitigate torsional oscillations using shunt converter phase angle as a control signal. A UPFC model based on the model that was proposed by Nabavi-Niaki and Iravani was introduced in [4], in order to incorporate it in Phillips-Heffron model of power system to study the UPFC capability to damp

power system oscillations.

Evolutionary optimization algorithms such as genetic algorithm (GA), particle swarm optimization (PSO), and imperialist algorithm (IA) , also known as a population based optimization. These type of algorithms, suggests a population of candidate solutions based on the constraints of the problem, and as time progresses, the population evolve to yield a better solution to that problem.

These algorithms proved to be a useful tool in many studies for designing FACTS based power oscillation damping (POD) controller, that provide good response characteristics. Sidhartha, et al in [8] designed a TCSC based power system stabilizer using GA. Abido, Al-Awami, and Abdel-Majed [9, 10, 2] introduced a comparison study between UPFC based POD and PSS, where both of the controller were designed using PSO. The study also investigated the controllability of the UPFC different input channel to damp power system oscillations. It was observed that the shunt converter phase angle provides better controllability for damping electromechanical oscillations compared to the other input channels. In [11], an output feedback UPFC POD controller, in which PSO was used to evaluate time based objective function in order to find the optimal gains for the controller. Similarly, chaotic optimization algorithm (COA) was used in [12] to design an output feedback UPFC controller. A lead-lag based POD controller was designed in [13], where IA was used to evaluate an eigenvalue damping ratio objective function was evaluated.

In this paper a biogeography based optimization (BBO) algorithm, a new population based algorithm, is considered to design a POD controller. BBO is used to evaluate an eigenvalue damping ratio based objective function in order to determine the optimal gain and time constants of a two stage lead-lag controller. The results were compared with a PSO based POD controller, in order to investigate its capability in finding the optimal controller parameters.

2 System Modeling

2.1 Power System and Unified Power Flow Controller Model

The system considered in this paper is illustrated in Figure.1, which shows a single machine infinite bus (SMIB) system with double transmission line circuits equipped with a UPFC. The UPFC consists of two three phase GTO based voltage source converters (VSC) connected back to back through a common DC link capacitor. The shunt converter or the excitation converter is coupled to the system through an excitation transformer (ET). The series converter or the boosting converter is coupled to the system through a boosting trasnformer(BT).

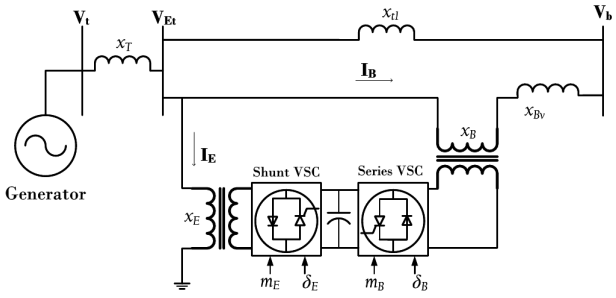

Figure 1: SMIB power system equipped with UPFC

By applying Park's transformation, and by neglecting the resistances and transients of the excitation and boosting transformers the UPFC can be modeled as[9, 7, 4]:

$$\begin{vmatrix} v_{Etd} \\ v_{Etq} \end{vmatrix} = \begin{vmatrix} 0 & x_E \\ -x_E & 0 \end{vmatrix} \begin{vmatrix} i_{Ed} \\ i_{Eq} \end{vmatrix} + \frac{m_E v_{dc}}{2} \begin{vmatrix} \cos\delta_E \\ \sin\delta_E \end{vmatrix} \quad (1)$$

$$\begin{vmatrix} v_{Btd} \\ v_{Btq} \end{vmatrix} = \begin{vmatrix} 0 & x_B \\ -x_B & 0 \end{vmatrix} \begin{vmatrix} i_{Bd} \\ i_{Bq} \end{vmatrix} + \frac{m_B v_{dc}}{2} \begin{vmatrix} \cos\delta_B \\ \sin\delta_B \end{vmatrix} \quad (2)$$

$$\begin{aligned} \frac{dv_{dc}}{dt} &= \frac{3m_E}{4C_{dc}} \begin{vmatrix} \cos\delta_E & \sin\delta_E \end{vmatrix} \begin{vmatrix} i_{Ed} \\ i_{Eq} \end{vmatrix} + \\ &\quad \frac{3m_B}{4C_{dc}} \begin{vmatrix} \cos\delta_B & \sin\delta_B \end{vmatrix} \begin{vmatrix} i_{Bd} \\ i_{Bq} \end{vmatrix} \end{aligned} \quad (3)$$

where
v_{Et}: Excitation transformer voltage
i_E: Excitation current
v_{Bt}: Boosting transformer voltage
i_B: Boosting current
C_{dc}: DC link capacitance
v_{dc}: DC link voltage The UPFC has four control input signals where m_E and δ_E are the excitation branch amplitude and phase angles respectively, and m_B and δ_B are the boosting branch amplitude and phase angle respectively.

The nonlinear model of the generator shown in figure 1 is given as:

$$\frac{d\delta}{dt} = \omega_B(\omega - 1) \quad (4)$$

$$\frac{d\omega}{dt} = \frac{1}{M}(-D(\omega - 1) + P_m - P_e) \quad (5)$$

$$\frac{dE'_q}{dt} = \frac{1}{T'_{do}}\left(-E'_q + E_{fd} - (x_d - x'_d)\, i_d\right) \quad (6)$$

$$\frac{dE_{fd}}{dt} = \frac{1}{T_A}(-E_{fd} + K_A(V_{ref} - V_t)) \quad (7)$$

where :
$P_e = v_d i_d + v_q i_q$, $v_q = E'q - x'_d i_d$, $v_d = x_q i_q$,$V_t = \sqrt{(v_d^2 + v_q^2)}$,

$i_d = i_{TLd} + i_{Ed} + i_{Bd}$, and $i_q = i_{TLq} + i_{Eq} + i_{Bq}$

From the above equations, the network currents can be rewritten as:

$$i_{TLd} = \frac{1}{x_{t1}}\left(x_E i_{Ed} + \frac{m_E v_{dc}}{2}\sin\delta_E - V_b\cos\delta\right) \quad (8)$$

$$i_{TLq} = \frac{1}{x_{t1}}\left(x_E i_{Eq} - \frac{m_E v_{dc}}{2}\cos\delta_E + V_b\sin\delta\right) \quad (9)$$

$$i_{Ed} = \frac{x_{BB}}{x_{d2}}E'_q + x_{d7}\frac{m_B v_{dc}}{2}\sin\delta_B + x_{d5}V_b\cos\delta + x_{d6}\frac{m_E v_{dc}}{2}\sin\delta_E \quad (10)$$

$$i_{E_q} = x_{q7}\frac{m_B v_{dc}}{2}\cos\delta_B + x_{q5}V_b\sin\delta + x_{q6}\frac{m_E v_{dc}}{2}\cos\delta_E \quad (11)$$

$$i_{Bd} = \frac{x_E}{x_{d2}}E'_q - \frac{x_{d1}}{x_{d2}}\frac{m_B v_{dc}}{2}\sin\delta_B + x_{d3}V_b\cos\delta + x_{d4}\frac{m_E v_{dc}}{2}\sin\delta_E \quad (12)$$

$$i_{Bq} = \frac{x_{q1}}{x_{q2}}\frac{m_B v_{dc}}{2}\cos\delta_B + x_{q3}V_b\sin\delta + x_{q4}\frac{m_E v_{dc}}{2}\cos\delta_E \quad (13)$$

where x_E and x_B represents the leakage reactances of ET and BT respectively, while x_{BB}, $x_{d1} - x_{d7}$, and $x_{q1} - x_{q7}$ are given in [10].

2.2 System Linearized Model

A linearised model is determined to suite the design approach considered in this paper. This is necessary to facilitate the assessment of the stability of the system, and to construct an objective function based on the system eigenvalues. For this purpose, the system is linearized around different operating points, and the linear model yield is given by:

$$\dot{x} = A\,x + B\,u \quad (14)$$

where x is the state vector and u is the input vector :

$$x = \begin{bmatrix}\Delta\delta & \Delta\omega & \Delta E'_q & \Delta E_{fd} & \Delta v_{dc}\end{bmatrix}^T \quad (15)$$

$$u = \begin{bmatrix}\Delta m_E & \Delta\delta_E & \Delta m_B & \Delta\delta_B\end{bmatrix} \quad (16)$$

where A and B are:

$$A = \begin{bmatrix} 0 & \omega_B & 0 & 0 & 0 \\ -\frac{K_1}{M} & -\frac{D}{M} & -\frac{K_2}{M} & 0 & -\frac{K_{pd}}{M} \\ -\frac{K_4}{T'_{do}} & 0 & -\frac{K_3}{T'_{do}} & \frac{1}{T'_{d0}} & -\frac{K_{qd}}{T'_{do}} \\ -\frac{K_A K_5}{T_A} & 0 & -\frac{K_A K_6}{T_A} & -\frac{1}{T_A} & -\frac{K_A K_{vd}}{T_A} \\ K_7 & 0 & K_8 & 0 & -K_9 \end{bmatrix} \quad (17)$$

$$B = \begin{bmatrix} 0 & 0 & 0 & 0 \\ -\frac{K_{pe}}{M} & -\frac{K_{p\delta e}}{M} & -\frac{K_{pb}}{M} & -\frac{K_{p\delta b}}{M} \\ -\frac{K_{qe}}{T'_{do}} & -\frac{K_{q\delta e}}{T'_{do}} & -\frac{K_{qb}}{T'_{do}} & -\frac{K_{q\delta b}}{T'_{do}} \\ -\frac{K_A K_{ve}}{T_A} & -\frac{K_A K_{v\delta e}}{T_A} & -\frac{K_A K_{vb}}{T_A} & -\frac{K_A K_{v\delta b}}{T_A} \\ K_{ce} & K_{c\delta e} & K_{cb} & K_{c\delta b} \end{bmatrix} \quad (18)$$

where $K_1 - K_9$, K_{pu},K_{qu}, and K_{cu} are the linearization constants.

2.3 UPFC - based Damping Controller

The structure of the POD controller is shown in Figure.2. It consists of a washout circuit which is provided to eliminate the steady state bias from the output of the damping controller, cascaded with lead-lag compensator.

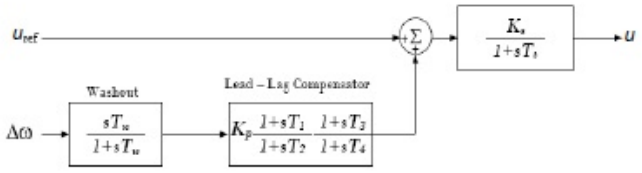

Figure 2: UPFC Based Damping Controller

The three term PID controllers, as dynamic compensator in power system stabilizers, is widely implemented in reducing system damping oscillations. . In [14], a PID controller design based on particle swarm optimization for a multimachine system were successfully implemented. In this paper the two stage lead-lag compensator is used. The transfer function of the two stages controller is given by:

$$T(s) = K_p\frac{(1+sT_1)}{(1+sT_2)}\frac{(1+sT_3)}{(1+sT_4)} \quad (19)$$

The control signal u of the UPFC can be any of the input signals m_E, δ_E, m_B,or δ_B. Based on [9, 10, 2], a singular variable decomposition was applied to measure the controllability of the electromechanical (EM) mode, and it was found that δ_E had the best controllability measurement compared to the other UPFC control signals. Thus it is logical to consider δ_E as the control signal when designing a damping controller.

2.4 Objective Function

2.4.1 Eigenvalue Damping Coefficients Based Objective Function

In this approach, the damping coefficients of the dominant eigenvalues are to be maximized.. Then the damping coefficient ζ_i of the i-th eigenvalue is defined through the following equation 20:

$$\zeta_i = -\frac{\alpha_i}{\sqrt{\alpha_i^2 + \beta_i^2}} \quad (20)$$

Where α_i and β_i are the real and imaginary parts of the dominant eigenvalue respectively. A system with a damping for all eigenvalues greater than 5% is considered to be a well damped power system [15]. Therefore, The problem is formulized such that to achieve a damping for all eigenvalues greater than 5% over the range of the operating points, by the optimization process.

Let Ξ_p be a vector of the damping factors of all eigenvalues of the p-th operating point in the set, where

$p = 1, 2, .., n$ for n operating points. Then the objective function to be maximized is:

$$\max\ J_e \tag{21}$$

where $J_e = \min(\min(\Xi_p))$

2.4.2 Time Based Objective Function

For a robust tuning using the ITAE criterion, the objective function for set of operating points is formulated as:

$$\min\ J_t \tag{22}$$

where:

$$J_t = \sum_{i=1}^{p} \left(\int t|\Delta\omega_i|dt \right) \tag{23}$$

To indirectly limit the control action of the resulting controllers from reaching saturation, both objective functions considered above are subjected to the following constraints:

$$\begin{aligned} K_{pmin} \leq K_p \leq K_{pmax} \\ T_{1mn} \leq T_1 \leq T_{1max} \\ T_{2min} \leq T_2 \leq T_{2max} \\ T_{3min} \leq T_3 \leq T_{3max} \\ T_{4min} \leq T_4 \leq T_{4max} \end{aligned} \tag{24}$$

In both cases only a DC voltage regulator is incorporated in the system in order to stabilize the DC link voltage. The parameters for the DC regulator are obtained beforehand and kept constant during the optimization process.

3 Optimization Algorithms

3.1 Biogeography Based Optimization

Biogeography-Based Optimization (BBO), introduced by Simon[16] is a population based stochastic based evolutionary algorithm. Based on island biogeography theory, that is the nature way to achieve optimal condition of life through the distribution of species among islands. This can be translated to a mathematical optimization problem, in which a number of candidate solutions referred to as population and each solution from the population is termed as an individual. An individual that performs well on the objective function is analogous to an island that attracts different spices and it is said to have high suitability index (HSI), and the individuals that perform poor on the objective function are analogous to low HSI islands where it attracts lower number of species.

The mathematical model of biogeography describes the immigration and emigration of species from an island. Islands with high HSI have high emigration rates and low immigration rates, due to the high population of species in that island. Low HSI islands have low emigration rates and high immigration rates and that is due to the large space and low species in these islands. The factors that characterize the HSI of an island are called suitability index variables (SIV), and the include vegetative diversity, rain fall, topographic diversity, land area and temperature.

If an optimization problem was to be solved using BBO, the independent variables of the problem are analogus to the SIV of an island, and the solutions for that proposed individual is the HSI of such an island. As in biogeography theory that high HSI islands having lower immigration rate thus it will be more reluctant to change than the low HSI islanfs having immigration rates. Therefore, a good individual will have low tendency to change than poor individuals. On the other hand, the high HSI islands have high emigration rate and hence tendency to share its features with the low HSI islands having low emigration rates. Thus, the good individuals will share its features with the poor individuals. The addition of new features to poor individuals may raise the quality of those individuals.

MacArthur and Wilson [17], has illustrated the model of species abundance on a single island as shown in figure (3). Immigration rate λ and emigration rates are functions of the number of species in the island.

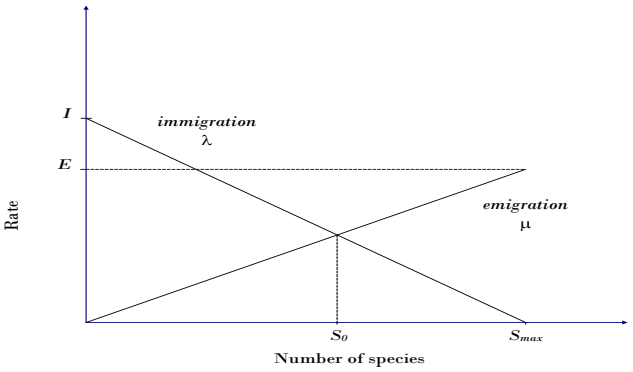

Figure 3: Species migration model of an island, based on [MacArthur and Wilson,1967[17]]

In BBO each individual is represented by an identical species count curve with $E = I$ for simplicity, as illustrated in figure (4). The migration model shown below is called a linear migration model where $\lambda$and $\mu$are both linear functions of the cost.

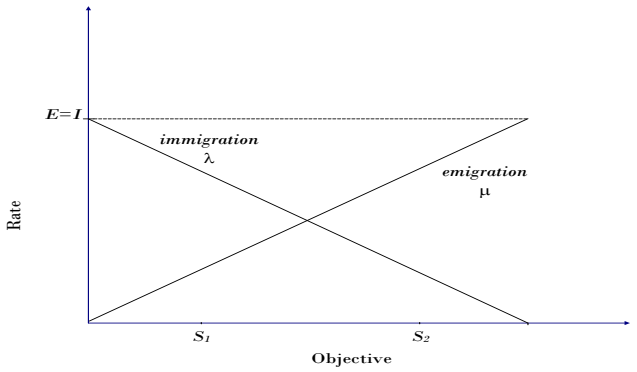

Figure 4: BBO individual species count curve with $E = I$

BBO has two major operations:

3.1.1 BBO Migration

Consider the following constrained optimization problem:

$$\min_{x \in \mathbb{R}^{\mathbf{n}}} f(\mathbf{x}) \tag{25}$$

where $x = [x_1, x_2, \cdots, x_n]^T$.

x would be an individual which is analogous to an island, and $x_1, x_2, \cdots, x_n$ would be analogous to SIV of an island. Hence when an migration occurs the SIV's of an island will either immigrate to the individual or the will emigrate from the individual. In BBO a use of migration rates of each individual to probabilistically share information between individuals. There are different ways to implement migration in BBO, but in this study the original BBO developed in [16] will be used which is referred to as partial immigration based.

Suppose that there are a population of size N and that x_k is the k-th individual in the population where $k \in [1, N]$, and the size of the optimization problem is n. $x_k(s)$ is the s-th independent variable in the individual, where $s \in [1, n]$. Based on the cost function evaluation the immigration probability λ_k, is given for the k-th individual and for all of its solution features $s \in [1, n]$, so in each generation there would be a probability of $\lambda_k$that this individual will be replaced.

Once a solution feature is selected to be replaced, then selection of the emigrating solution feature is done based on the emigrating probability of that individual $\{\mu_i\}$.

3.1.2 BBO Mutation

In BBO there are two main operators , i.e, migration and mutation. Simon [16], has referred to mutation of SIV to be analogous to the introduction of an excursion to a habitat that will drive it away from its equilibrium point and that can happen randomly. An example is the arrival of large piece of flotsam to the island. Mutation rates are determined through the species count probabilities using equation (26).

$$\dot{P}_s = \begin{cases} -(\lambda_s + \mu_s) P_s + \mu_{s+1} P_{s+1} & S = 0 \\ -(\lambda_s + \mu_s) P_s + \lambda_{s-1} P_{s-1} + \mu_{s+1} P_{s+1} & 1 \leq S \leq S_{max} - 1 \\ -(\lambda_s + \mu_s) P_s + \lambda_{s-1} P_{s-1} & S = S_{max} \end{cases} \tag{26}$$

From figure (4), it can be seen that for low species count and high species count both have relatively low probabilities. While for medium species count they have high probabilities for change as they are near the equilibrium point.

The mutation rates can be found as:

$$m_i = m_{max} \left(1 - \frac{P_i}{P_{max}} \right) \tag{27}$$

where

m_i : the i-th individual mutation rate

m_{max} : the maximum mutation rate, typical between and.

P_i : i-th individual species count probability

P_{max} : Maximum species count probability from all individuals

3.2 Particle Swarm Optimization

Particle swarm optimization (PSO) was introduced by Kennedy and Eberhart in 1995, [18]. PSO is a population based iterative search algorithm that manipulates a number of candidate solutions, referred to as particles, in order to find the optimum. The PSO was discovered through simulation of simple social models. It imitates the swarm behavior such as birds flocking and fish schooling, and this behavior is referred to as swarm intelligence[19].

This algorithm searches the space of an objective function by adjusting the trajectories of individual particles, as these trajectories form piecewise path in a quasi-stochastic manner. The movement of a swarming particles consists of two major components: stochastic component and a deterministic component. Each particle is attracted toward the position of the current global best g_{best} and it own personal best location p_{best} in history, while in the same time it has tendency to move randomly [19].

4 Simulation Results

The above two objective functions were considered in the design process of UPFC based damping controller with 30 different operating conditions. The resulting four controllers were then tested at 4 different loading conditions

of the system, with different system uncertainties given in table 1, to investigate system robustness.

Table 1: Controller testing loading conditions with system uncertainties

Loading Condition	P_e	Q_e	System Parameter uncertainty
Light	0.30	0.015	30% increase in line reactance x_{t1}
Nominal	1.0	0.015	No parameter uncertainty
Heavy	1.1	0.4	25% increase in machine inertia M
Leading power factor	0.7	-0.03	30% increase in field time constant T'_{do}

For both objective functions and for the two optimization algorithms, the initialization was performed with 100 generations and a population of 100 individuals. The maximum mutation rate for BBO was set to be 0.005 while the acceleration coefficients for PSO c1 = c2 = 2.05, where the inertia weighting was set as linear function of the generation as it decreases from 0.9 to 0.4 during generation progress.

Figures 5 and 6, illustrates the convergence characteristics of the two optimization algorithms for the two objective functions:

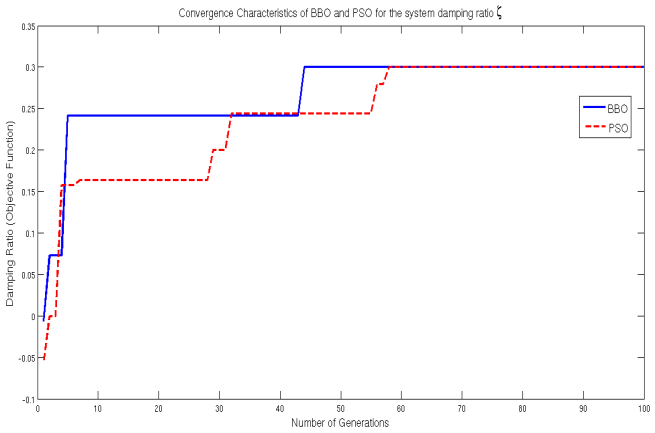

Figure 5: Convergence characteristics of BBO and PSO for a ζ - based objective function

The obtained parameters of the damping controller for each case is given in table 2 below:

The controllers were tested for a 10% step increase in generator mechanical input power P_m at the four loading condition mentioned in table 1.

4.1 Controller Characteristics

As mentioned above that the POD controller is a lead lag compensator, where the structure of the controller is given in figure 19. Each controller will have two real zeros and two real poles, and they are given in table 3:

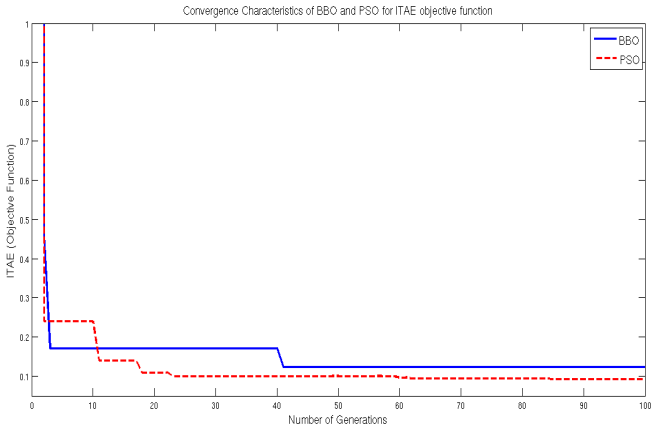

Figure 6: Convergence characteristics of BBO and PSO for ITAE based objective function

Table 2: Optimal parameter setting of the damping controller using BBO and PSO for the two objective function

	BBO		PSO	
	damping Based	ITEA - Based	damping Based	ITAE - Based
K_p	-98.5099	-94.8712	-89.8943	-98.9509
T_1	1.0814	0.0143	0.0578	1.4550
T_2	0.5190	0.3284	0.6519	0.6472
T_3	0.0520	0.7778	1.4808	0.0544
T_4	0.6451	0.7126	0.6807	0.7519
J	0.3005	0.3003	0.1231	0.0920

Table 3: POD controllers poles and zeros

	Controller poles (p)	Controller zeros (z)
BBO damping based	p_1= 1.9268	z_1= -0.9247
	p_2=1.5501	z_2= -19.2307
PSO damping based	p_1= -1.5340	z_1= -17.3010
	p_2=-1.4690	z_2= -0.6753
BBO ITAE based	p_1= -3.045	z_1=-69.9300
	p_2=-1.4033	z_2= -1.2856
PSO ITAE based	p_1= -1.5451	z_1=-0.6873
	p_2=-1.3300	z_2= -18.3824

The controllers frequency responses are illustrated in figure 7. It can be observed that the lag part of the controller dominates at low frequencies and exhibits magnitude response similar to that of a lag compensator. The controllers suppress the high frequency components of the signal (transient phase) and increase loop gain, and which is in line with the objective of smoothening and damping the low frequency oscillations and improve the steady state response. Thus, as the lag action is dominant, it acts as and mimics the behavior of an integral

action of the PID controller, and hence eliminating the steady state error.

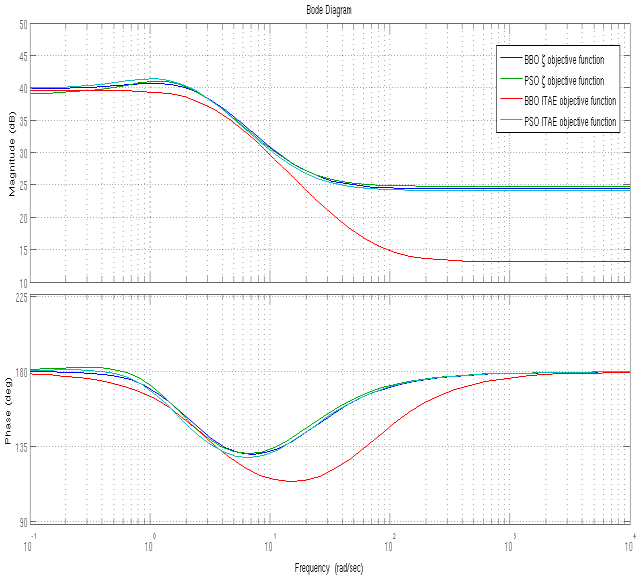

Figure 7: Controllers magnitude and phase responses

4.2 Light Loading

The system response for the disturbance under generator light loading condition with system uncertainty (30% increase in x_{t1}) for the four controllers is given in figures 8 to 10:

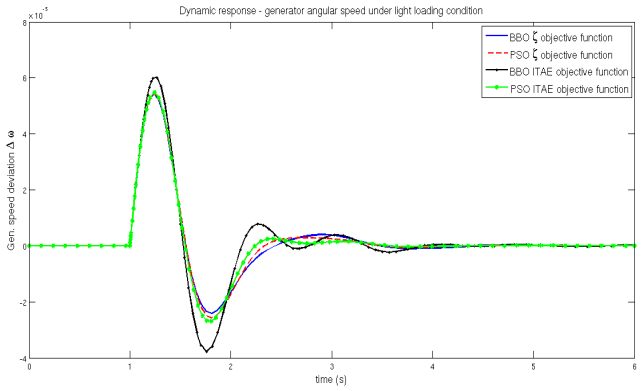

Figure 8: System dynamic response under light loading - Deviation in rotor angular speed $\Delta\omega$

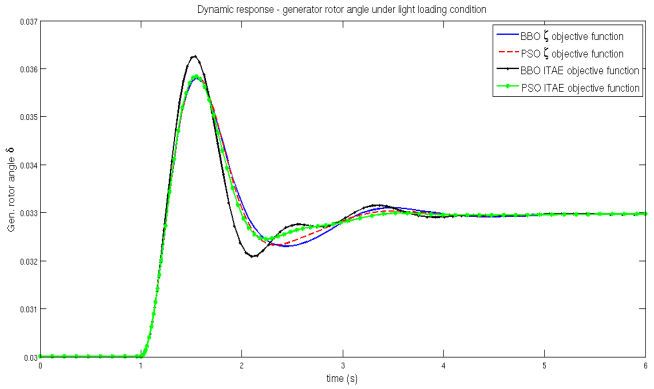

Figure 9: System dynamic response under light loading - Generator rotor angle δ

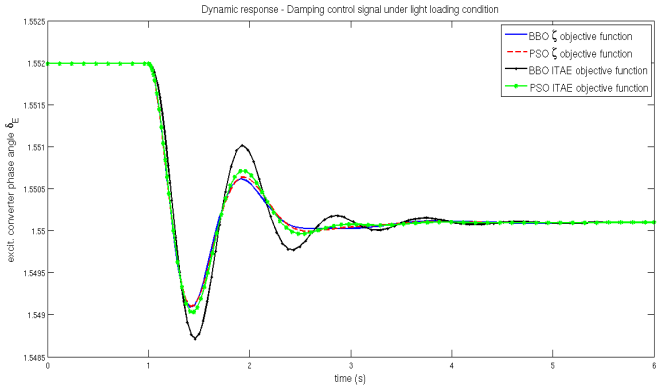

Figure 10: System dynamic response under light loading - UPFC excitation converter phase angle δ_E (control signal)

The responses of the controllers are illustrated in table 4:

It is evidence that the BBO ITAE based controller has the lowest settling time from table4 compared to the other controllers. On the other hand, it can be seen from figures 8 to 9 ,that the system response exhibits transient oscillations with this controller, which is due to the low damping coefficient ζ of the system.

4.3 Nominal Loading

Figures 11 to 13, illustrates the system response of the tuned controllers under nominal loading conditions. The system is simulated for a 10% step change disturbance in P_m with no parameter uncertainties introduced.

Table 4: System performance under light loading

	Settling time t_s	Maximum peak (M_p)	EM modes and damping ζ
BBO damping based	1.1470	0.0005	mode $=-2.75 \pm j6.93$ $\zeta = 0.3685$
PSO damping based	1.1206	0.0005	mode $=-2.72 \pm j6.51$ $\zeta = 0.3861$
BBO ITAE based	1.0305	0.0006	mode = $-1.57 \pm j7.05$ $\zeta = 0.2178$
PSO ITAE based	1.0820	0.0005	mode $=-2.36 \pm j6.50$ $\zeta = 0.3410$

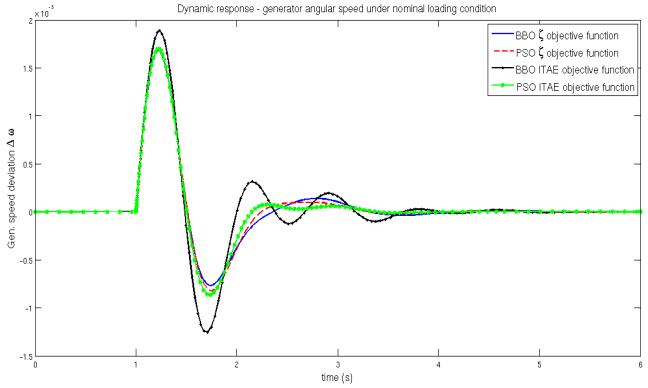

Figure 11: System dynamic response under nominal loading - Deviation in rotor angular speed $\Delta\omega$

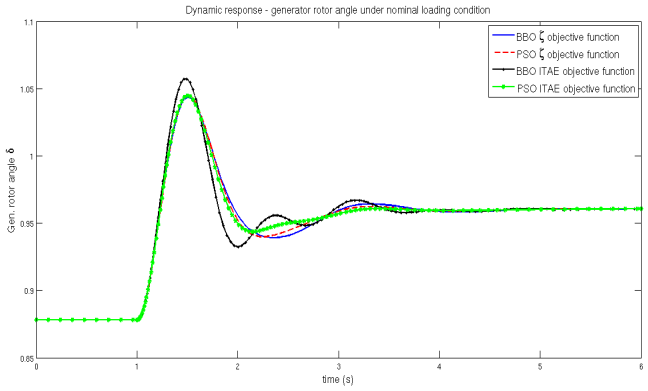

Figure 12: System dynamic response under nominal loading - Generator rotor angle \delta

The controllers performance characteristics are given in table 5:

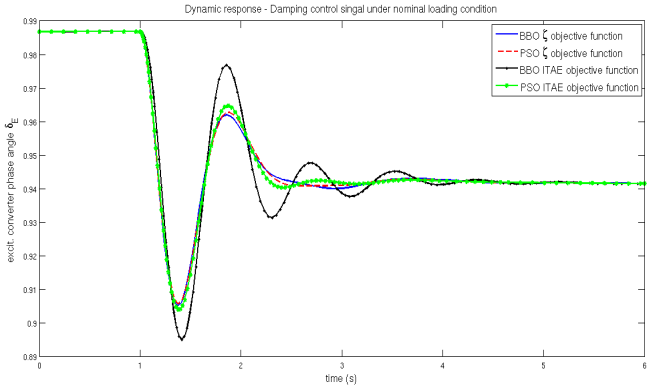

Figure 13: System dynamic response under nominal loading - UPFC excitation converter phase angle δ_E

Table 5: System performance under nominal loading

	Settling time t_s	Maximum peak (M_p)	EM modes and damping ζ
BBO damping based	2.0067	0.0017	mode $=-2.84 \pm j7.35$ $\zeta = 0.3608$
PSO damping based	1.1739	0.0017	mode $=-2.85 \pm j6.88$ $\zeta = 0.3831$
BBO ITAE based	2.0790	0.0019	mode = $-1.46 \pm j7.48$ $\zeta = 0.1911$
PSO ITAE based	1.1143	0.0017	mode $=-2.44 + j6.87$ $\zeta = 0.3342$

Figures 11 and 12 show the system response under nominal loading for all of the controllers, where figure 13 shows the control signal δ_E to the system. It can be seen the BBO ITAE based controller has the lowest performance compared to other schemes, the highest settling time and lowest damping factor ζ which is translated as an oscillatory system response. On the other hand, the PSO based controllers, ITAE and the damping based, has the best system performance compared to the BBO based controllers.

4.4 Heavy Loading

In Figures 14 and 15 the system response for a 10% step change in input mechanical power P_m under heavy loading with a 25% change in the moment of inertia of the generator M are shown. Figure 16, illustrates the controller output signal δ_E, which is the phase angle of the excitation converter of the UPFC.

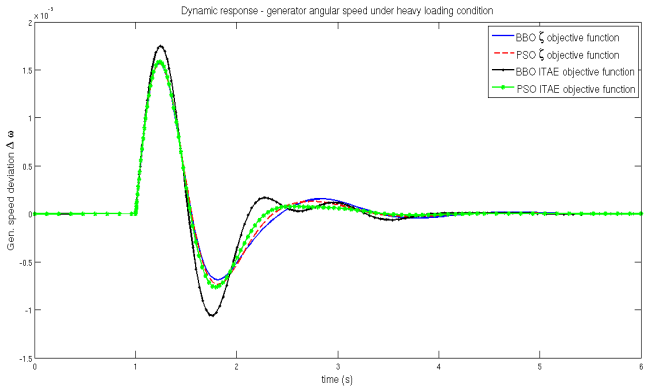

Figure 14: System dynamic response under heavy loading - Deviation in rotor angular speed $\Delta\omega$

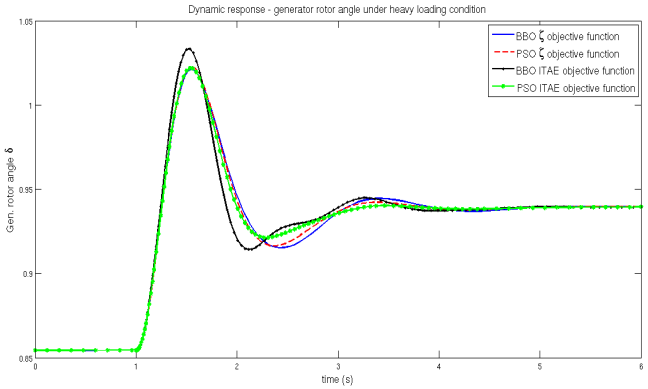

Figure 15: System dynamic response under heavy loading - Generator rotor angle δ

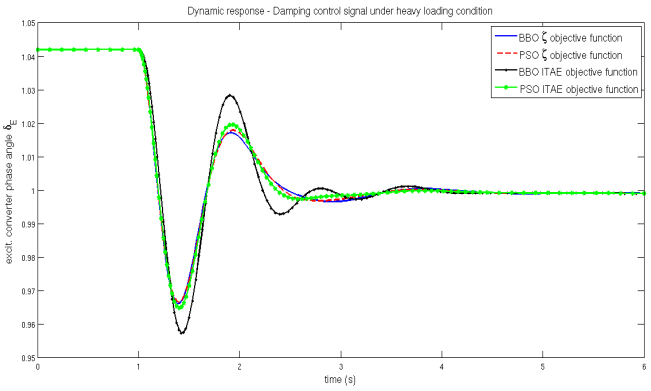

Figure 16: System dynamic response under heavy loading - UPFC excitation converter phase angle δ_E

The controllers performance criteria are given in table 6:

From the system responses in figures 14 and 15 and from table 6, it can be seen that PSO tuned controllers yield a better performance in terms of the damping and settling time when compared with BBO tuned controllers. Moreover, the BBO ITAE tuned controller has less settling than the BBO damping based tuned controller, however the damping based controller has greater damping factor as evident from the system response where the BBO ITAE tuned controller has some oscillations before settling to zero.

Table 6: System performance under heavy loading

	Settling time t_s	Maximum peak (M_p)	EM modes and damping ζ
BBO damping based	2.1244	0.0016	mode $=-3.07 \pm j6.94$ $\zeta = 0.3702$
PSO damping based	1.9833	0.0016	mode $=-3.08 + j6.44$ $\zeta = 0.4279$
BBO ITAE based	2.0952	0.0017	mode $=-1.76 \pm j7.09$ $\zeta = 0.2403$
PSO ITAE based	1.2239	0.0016	mode $=-2.65 \pm j6.40$ $\zeta = 0.3823$

4.5 Leading Power Factor Loading

Under leading power factor loading condition ($P_e = 0.7$p.u, $Q_e = -0.03$ p.u), the system is disturbed by a 10% step change in P_m. The results that were obtained for the system response for each of the designed controller are given in figures 17 and 18. The controller action is also given in figure 19.

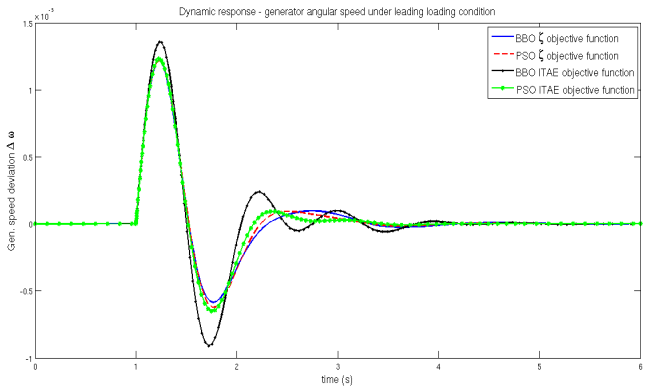

Figure 17: System dynamic response under leading loading - Deviation in rotor angular speed $\Delta\omega$

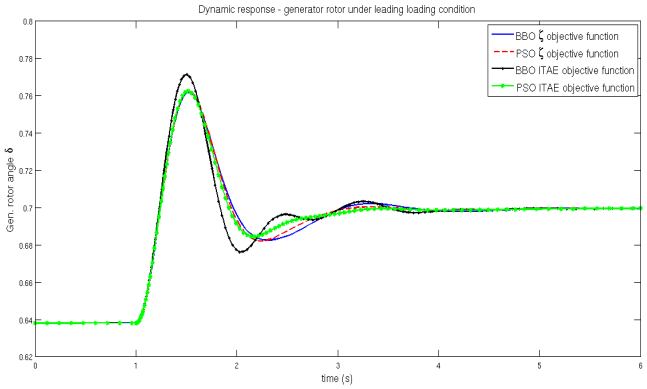

Figure 18: System dynamic response under leading loading - Generator rotor angle δ

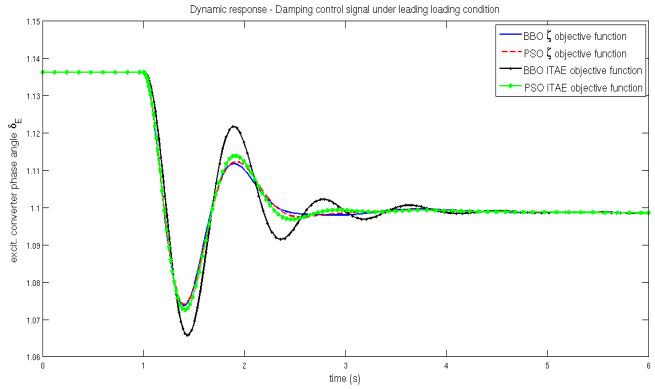

Figure 19: System dynamic response under leading loading - UPFC excitation converter phase angle δ_E

The controllers performance are given in table 7:

Table 7: System performance under leading loading

	Settling time t_s	Maximum peak (M_p)	EM modes and damping ζ
BBO damping based	1.2105	0.0012	mode $=-2.82 \pm j6.94$ $\zeta = 0.3769$
PSO damping based	1.1702	0.0012	mode $=-2.78 \pm j6.44$ $\zeta = 0.3955$
BBO ITAE based	1.3993	0.0014	mode $=-1.52 \pm j7.14$ $\zeta = 0.2084$
PSO ITAE based	1.1020	0.0012	mode $=-2.35 \pm j6.48$ $\zeta = 0.3405$

From the results obtained from the simulation, it can be seen that PSO tuned controllers are superior to the BBO tuned controllers in terms of damping and settling time.

5 Conclusion

This paper presented a comparison study between two evolutionary optimization algorithms, namely, biogeography based optimization (BBO) and particle swarm optimization (PSO) , in designing a UPFC based power oscillation damping controller. The designed POD controllers were tuned via two different objective functions, the eigenvalue damping factor based objective function, and the ITAE based objective function. It was shown that the performance of algorithms vary based on the objective function used, where for a damping factor based objective function the performance of BBO and PSO is almost similar. On the other hand, the performance of the algorithms varied for the ITAE based objective function where PSO showed a better performance compared to BBO. The yielded controllers are then compared based on the controlled system characteristics and the performance. To assess the robustness of the resulting controllers, system is simulated for different generator loading conditions. The controllers were able to maintain the stability of the system at each of the loading conditions, with some variation in the performance for each case.

System Data

Generator Data: $x_d = 1$; $x_q = 0.3$; $x'_d = 0.3$; $D = 0$; $M = 10$; $T'_{do} = 5.044$; $\omega_B = 100\pi$; $V_t = 1.05$
Transmission line: $x_T = 0.1$; $x_{t1} = 0.6$;$x_{Bv} = 0.6$
UPFC : $x_E = 0.1$; $x_B = 0.1$; $C_{dc} = 3$; $V_{dc} = 2$; DC voltage regulator: $k_{di} = -0.10$; $k_{dp} = -6.05$

References:

[1] K. Padiyar, *Power system dynamics*. BS publications, 2008.

[2] A. T. Al-Awami, M. A. Abido, and Y. L. Abdel-Magid, "Application of pso to design upfc-based stabilizers."

[3] A. Rahim and S. Nassimi, "Synchronous generator damping enhancement through coordinated control of exciter and svc," *IEE Proceedings-Generation, Transmission and Distribution*, vol. 143, no. 2, pp. 211–218, 1996.

[4] H. Wang, "A unified model for the analysis of facts devices in damping power system oscillations. iii. unified power flow controller," *Power Delivery,*

IEEE Transactions on, vol. 15, no. 3, pp. 978–983, Jul 2000.

[5] M. Abido, "Power system stability enhancement using facts controllers: A review." *Arabian Journal for Science & Engineering (Springer Science & Business Media BV)*, vol. 34, 2009.

[6] ——, "Analysis and assessment of statcom-based damping stabilizers for power system stability enhancement," *Electric Power Systems Research*, vol. 73, no. 2, pp. 177–185, 2005.

[7] A. Nabavi-Niaki and M. Iravani, "Steady-state and dynamic models of unified power flow controller (upfc) for power system studies," *Power Systems, IEEE Transactions on*, vol. 11, no. 4, pp. 1937–1943, Nov 1996.

[8] S. Panda and N. P. Padhy, "Matlab/simulink based model of single-machine infinite-bus with tcsc for stability studies and tuning employing ga." *International Journal of Computer Science & Engineering*, vol. 1, no. 1, 2007.

[9] M. A. Abido, A. Al-Awami, and Y. Abdel-Magid, "Analysis and design of upfc damping stabilizers for power system stability enhancement," in *Industrial Electronics, 2006 IEEE International Symposium on*, vol. 3, July 2006, pp. 2040–2045.

[10] M. Abido, A. T. Al-Awami, and Y. Abdel-Magid, "Simultaneous design of damping controllers and internal controllers of a unified power flow controller," in *Power Engineering Society General Meeting, 2006. IEEE*. IEEE, 2006, pp. 8–pp.

[11] H. Shayeghi, H. Shayanfar, S. Jalilzadeh, and A. Safari, "Design of output feedback upfc controller for damping of electromechanical oscillations using pso," *Energy Conversion and Management*, vol. 50, no. 10, pp. 2554–2561, 2009.

[12] ——, "Coa based robust output feedback upfc controller design," *Energy Conversion and Management*, vol. 51, no. 12, pp. 2678–2684, 2010.

[13] A. Ajami and R. Gholizadeh, "Optimal design of upfc-based damping controller using imperialist competitive algorithm," *Turkish Journal of Electrical Engineering & Computer Sciences*, vol. 20, no. Sup. 1, pp. 1109–1122, 2012.

[14] A. Oonsivilai and B. Marungsri, "Stability enhancement for multi-machine power system by optimal pid tuning of power system stabilizer using particle swarm optimization," *WSEAS transactions on power systems*, vol. 3, no. 6, pp. 465–474, 2008.

[15] G. Rogers, *Power system oscillations*. Kluwer Academic Boston, 2000.

[16] D. Simon, "Biogeography-based optimization," *Evolutionary Computation, IEEE Transactions on*, vol. 12, no. 6, pp. 702–713, 2008.

[17] R. H. MacArthur, *The theory of island biogeography*. Princeton University Press, 1967, vol. 1.

[18] J. Kennedy, R. Eberhart *et al.*, "Particle swarm optimization," in *Proceedings of IEEE international conference on neural networks*, vol. 4, no. 2. Perth, Australia, 1995, pp. 1942–1948.

[19] X.-S. Yang, *Engineering optimization: an introduction with metaheuristic applications*. John Wiley & Sons, 2010.